# Level spin for superdeformed nuclei near $A=194$

J. A. Becker, E. A. Henry, A. Kuhnert, T. F. Wang, and S. W. Yates*
*Lawrence Livermore National Laboratory, Livermore, California 94550*

R. M. Diamond, F. S. Stephens, J. E. Draper,† W. Korten,‡ M. A. Deleplanque, A. O. Macchiavelli,§ F. Azaiez,** and W. H. Kelly††
*Lawrence Berkeley Laboratory, Berkeley, California 94720*

J. A. Cizewski and M. J. Brinkman
*Rutgers University, New Brunswick, New Jersey 08903*
(Received 28 August 1991)

Transition energies of 25 superdeformed (SD) bands in 13 nuclei of the $A=194$ region were fitted by the power-series expansion of $I$ in odd powers of $E_\gamma/2$, $\hbar(I+\frac{1}{2})=2\alpha\omega+\frac{4}{3}\beta\omega^3$, where $E_\gamma/2=\hbar\omega$, and by the expression for transition energy, $E_\gamma=E(I+2)-E(I)$, where $E(I)=AI(I+1)+B[I(I+1)]^2+C[I(I+1)]^3$. Results are generally similar, and level spins for these SD bands are given based on expectations of rotational model behavior.

PACS number(s): 21.10.Re, 21.60.Ev, 27.80.+w

## I. INTRODUCTION

The notion that reliable spin assignments may be made for superdeformed (SD) bands in the $A=194$ region based on expectations of the rotational model was introduced by Becker *et al.* [1] when they reported observation of superdeformation in $^{192}$Hg. All experimental evidence suggested that the SD band members in this mass region are nuclear states characterized by the dynamics of an extremely good quantum rotor. The first 11 observed transitions of the SD $^{192}$Hg cascade follow rotational model formulas with only a first-order correction. This is exceptional behavior among nuclear $\gamma$-ray cascades. For example, only the first four transitions in normally deformed $^{168}$Er show similar behavior. The SD transitions have large transition quadrupole moments $Q_t$. Moore *et al.* [2] measured $\bar{Q}_t[^{191}\mathrm{Hg}]\sim 18(3)$ *e* b, which corresponds to a deformation parameter $\beta=0.56$ and to transition strengths $B(E2)\sim 2000$ Weisskopf units (W.u.). Subsequently, $\bar{Q}_t=20(2)$ *e* b was measured [3] for nine transitions in $^{192}$Hg. Other features of the SD cascades suggested that application of the rotational model formulas might lead to reliable spin assignments. The change in $E_\gamma$ with increasing $\gamma$-ray energy has a smooth variation over the energy range observed, and the energy spectrum can be parametrized by a power expansion including only a first-order correction, in general. The intraband $\gamma$-ray transitions are observed down to low transition energies. The fractional change in $E_\gamma$ with $E_\gamma$ is largest and most sensitive to level spin at low spin, since $\Delta E_\gamma/E_\gamma\sim\Delta I/I$. In addition, it is unlikely that irregular behavior (e.g., unusual backbending) will occur in the low-energy region of the band since the Coriolis effects are small there. It is even more unlikely that irregular behavior occurs *entirely* below the lowest observed energy data point. Numerically, the cascades include enough transitions so that least-squares procedures can be followed.

These conditions were observed in many of the SD bands observed throughout the $A=194$ region, and so subsequently this notion was applied [4] to 16 SD bands in 9 nuclei near $A=194$. Measured cascade energies were compared to the rotational model expression: $\hbar(I+\frac{1}{2})=2\alpha\omega+4/3\beta\omega^3$, with $\hbar\omega\equiv E_\gamma/2$. Excellent fits to the data (measured by the goodness-of-fit parameter $\chi^2$) were reported, and a summary of the fitting parameters for the 16 SD bands known was given in Table I of Ref. [4]. The resulting ratio of expansion coefficients and the broad frequency range (large number of transitions) satisfactorily described by this equation confirm that these nuclei are excellent rotors. Level spins extracted from these fits are consistent with those inferred from yrast-state population in the SD band decay (where measured), after making an assumption about the angular momentum carried away by the unobserved linking transitions, typically 1–2 units.

These spin assignments have led to the surprising observation that alignment with respect to either $^{192}$Hg or $^{193}$Tl is quantized at $1\hbar$ for many of these bands [5–7], suggesting that pseudospin symmetry and triplet pairing

*Permanent address: University of Kentucky, Lexington, KY 40506.
†Permanent address: University of California, Davis, CA 95616.
‡Present address: Niels Bohr Institute, Copenhagen, Denmark.
§On leave from Comisión Nacional de Energia Atómica, Buenos Aires, Argentina.
**Present address: IPN-Orsay, F-91406, Orsay, France.
††Permanent address: Iowa State University, Ames, IA 50011.

might be important for bands in these nuclei. Consideration of these issues is on a firmer basis in this mass region than for nuclei near $A=152$ because spin assignments can be included in the discussion. Criticisms have been made for both the method and the physics, and therefore we review in Sec. II the rotational model formulas applied in this work to the transitions of the SD cascades. We discuss the relationship between the expansion of $I$ in powers of $\omega$ and the formula for $E$ as a power series in $I(I+1)$, $E=E_0+AI(I+1)+\cdots$, and the associated formula for transition energy, $E_\gamma$. In Sec. III, we discuss data selection, and then describe numerical results of the least-squares fits to rotational model formulas in more detail than given in Ref. [4]. A discussion of the fitting results is given for $^{192}$Hg, $^{194}$Hg, and $^{191}$Hg because different numerical results and spin assignments have been given by Wu, Feng, and Guidry [8,9] and by Wyss and Pilotte [10]. Tables of parameters obtained with two approaches, viz., the fitting parameters resulting from least-squares fits of observed transition energies to expansions of (i) $I$ in odd powers of $\omega$ ($E_\gamma=2\hbar\omega$), and (ii) $E_\gamma$ in powers of $I(I+1)$, are presented. Results for the two fitting equations are compared in Sec. IV. Spins are suggested for the SD band members based on identification of the spin parameter of the least-squares fitting equation with level spin in Sec. V. Uncertainties in these spin assignments are discussed. Some remarks on alignment are given in Sec. VI. Finally, a summary is presented in Sec. VII.

## II. ROTATIONAL MODEL EXPECTATIONS

### A. Rotational model formulas

The general reference for the rotational model formulas needed to relate the observed transition energies of the rotational cascade to level spin $I$ is Bohr and Mottelson (BM) [11]. The expression for the rotational energy of an axially symmetric ($K=0$) deformed nucleus in terms of rotational angular momentum is

$$E=\frac{\hbar^2}{2\mathcal{J}}I(I+1)\ . \tag{1}$$

Including higher-order correction terms to account for Coriolis coupling and other spin-dependent effects, the expression becomes

$$E(I)=AI(I+1)+BI^2(I+1)^2+CI^3(I+1)^3+\cdots\ . \tag{2}$$

The deviation from the leading-order term may be viewed as the consequence of a moment of inertia which is angular momentum dependent,

$$\mathcal{J}=\frac{\hbar^2}{2}[A+BI(I+1)+\cdots]^{-1}\ . \tag{3}$$

The expression for the rotational energy $E(K,I)$ with $K\neq0$ takes a form similar to Eq. (2), but includes a bandhead energy, and $I(I+1)$ is replaced by $I(I+1)-K^2$. A leading-order correction term occurs only for $K=\frac{1}{2}$ bands. Correction terms for $K>\frac{1}{2}$ bands are typically small and multiply powers of $I(I+1)$.

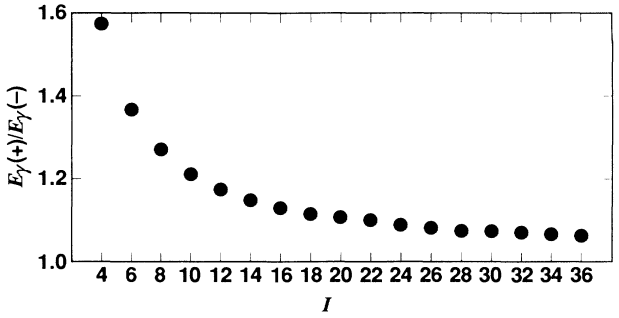


FIG. 1. The ratio $E_\gamma(+)/E_\gamma(-)=E_\gamma(I+2\rightarrow I)/E_\gamma(I\rightarrow I-2)$ for a rigid rotor.

The expression for the transition energy is given by

$$E_\gamma(I+2\rightarrow I)=E(I+2)-E(I)\ . \tag{4}$$

Direct substitution shows that the leading-order term for $E_\gamma$ is independent of $K$, except for $K=\frac{1}{2}$ bands.

### B. Sensitivity of spin to transition energy

The simplest rotational model formula predicts that $\Delta E_\gamma/E_\gamma\approx\Delta I/I$ within a band, which means the fractional change in $\gamma$-ray energy is largest at the low-spin end of the band. Thus, for a given statistical uncertainty in the measurements, the best measure of spin is obtained when the data extend to low $\gamma$-ray transition energies and to the corresponding low spins.

This sensitivity is illustrated in Fig. 1, where the ratio $E_\gamma(I+2\rightarrow I)/E_\gamma(I\rightarrow I-2)$, computed from Eqs. (1) and (4) for the rigid rotor, is presented as a function of $I$. [This ratio is $1+\Delta E_\gamma/E_\gamma(I\rightarrow I-2)$.] The ratio clearly increases with decreasing spin, and at $I=10$ the change in the ratio with 2 units of change in spin is well beyond the error of the $\gamma$-ray energy measurements, $\sim\frac{1}{4}\%$ for $E_\gamma$. As an example, the lowest $\gamma$-ray energy observed [12,13] in $^{194}$Pb is 169.7(2) keV, and the corresponding $\Delta E_\gamma=43.6(7)$ keV. Direct substitution into the expression above for $\Delta E_\gamma/E_\gamma$ gives, with $\Delta I=2$, $I\sim7.8(1)\hbar$ or $\sim5.8(1)\hbar$ for the spin of the final level of the 169.7-keV transition. This suggests that a first estimate of level spin can be made from the two cascade transitions lowest in energy. Such estimates are given in Sec. IV.

## III. THE LEAST-SQUARES FITS

### A. The data

Currently 27 SD bands in 13 nuclei have been reported in the $A=194$ region. The reference list presented in Ref. [4] included 16 SD bands in 9 nuclei. New experimental data reported since then include the following: Drigert *et al.* [14] have found evidence for a SD band in $^{189}$Hg. The number of bands in $^{193}$Hg has been extended to four, two of which exhibit backbending [15]. Superdeformation has been reported in two more isotopes of Pb, $^{192}$Pb (Ref. [16]) and $^{198}$Pb (Ref. [7]). Azaiez *et al.* [7] have reported four additional bands in $^{194}$Tl for a total of

six bands in that nucleus, and subsequently reported [18] two bands in $^{195}$Tl. All these data were fit except for the two bands in $^{193}$Hg which show backbending, and therefore cannot be fit with only first-order correction terms. In general, for the bands we consider: (i) $E_\gamma$ extends from $\sim$200 to $\sim$600 keV, (ii) at least nine $\gamma$ rays are included in the cascade, (iii) the difference in $E_\gamma$ for adjacent transitions ($\Delta E_\gamma$) decreases smoothly from $\sim$40 to 36 keV with increasing $E_\gamma$, and (iv) the fractional error in $E_\gamma$ is $\sim 10^{-3}$.

The energies of the nine $\gamma$-ray transitions lowest in energy were fit for each SD band. A fixed number of transitions was chosen to avoid data selection bias. Reported transitions lowest in energy were always included since $\Delta E_\gamma / E_\gamma$ is largest at low spin, as discussed above in Sec. II, and nine transitions were included after a preliminary survey of the data suggested that in this case the energy dependence of all the known bands could be fit by expansions which included only a first-order correction term. We also found that a good fit (measured by $\chi^2$) was not always obtained for some of the bands when reported uncertainties in transition energies were used in the fit, and that the quality of the fit was not improved by adding another term to the expansion. Our own experience with these measurements is that the uncertainty quoted in $E_\gamma$ is often too small. The experimental difficulty in locating the SD bands is well known. The band intensity represents 1% or less of the cross section, and in most instances, the SD cascade does not show up as distinct peaks in the projection of the 2D data matrix, $E_\gamma$ vs $E_\gamma$, onto one axis. Often only one "clean gate" can be set on the matrix to highlight the SD cascade. Experimentalists illustrate SD bands with $\gamma$-ray spectra from which background has been subtracted, and the experimental reports are not always clear as to whether or not the quoted uncertainty in $E_\gamma$ includes a contribution from uncertainty in the background subtraction. Therefore the following procedure was adopted when $\chi^2/\nu > 1$: quoted errors were multiplied by a factor $k$ (of order unity) in order to produce a fit with $\chi^2/\nu$ near 1. The $k$ factors are summarized in Table I, which will be discussed in detail subsequently. Fitting parameters and discussions given

TABLE I. Parameters from the least-squares fit of transitions 1–9 (beginning with the lowest energy) to $\hbar(I+\frac{1}{2})=2\alpha\omega+\frac{4}{3}\beta\omega^3$, where $\hbar\omega=E_\gamma/2$ [Eq. (5)]. All transitions are taken as $\Delta I=L=2$, and $I_f$ is the least-squares parameter corresponding to the final-state spin of transition 1. The asterisk indicates that only transitions 1–5 were used in the fit. Errors in the least-squares fitting parameters in this table and throughout the text represent the larger of the standard deviation $\sigma$ or uncertainty $[\approx(\chi^2/\nu)^{1/2}\sigma]$, in an effort to account for the scatter of the data. $\Delta = I_f -$ nearest (half-) integer.

| $^AZ$ | $E_\gamma$ (keV) | $10^2\alpha$ ($\hbar^2$/keV) | $10^8\beta$ ($\hbar^2$/keV$^3$) | $I_f$ ($\hbar$) | $\Delta$ ($\hbar$) | Ref.[a] | $k$[b] |
|---|---|---|---|---|---|---|---|
| $^{189}$Hg(1) | 366.0(4) | 4.373(63) | 5.58(51) | 14.96(10) | +0.46(10) | [14] | 1.0 |
| $^{189}$Hg(1*) | 366.0(4) | 4.327(180) | 6.06(183) | 14.83(52) | +0.33(52) | [14] | 1.0 |
| $^{190}$Hg(1) | 360.0(2) | 4.178(31) | 8.14(23) | 14.16(10) | +0.16(10) | [14] | 1.5 |
| $^{191}$Hg(1) | 350.6(1) | 4.558(22) | 5.62(17) | 14.87(7) | +0.37(7) | [2] | 2.0 |
| $^{191}$Hg(1*) | 350.6(1) | 4.728(78) | 3.75(85) | 15.34(22) | −0.16(22) | [2] | 2.0 |
| $^{191}$Hg(2) | 292.0(2) | 4.689(26) | 5.45(59) | 12.43(7) | −0.07(7) | [24] | 1.4 |
| $^{191}$Hg(3) | 311.8(4) | 4.662(42) | 6.45(35) | 13.38(13) | −0.12(13) | [24] | 1.4 |
| $^{192}$Hg(1) | 214.6(3) | 4.410(8) | 8.44(11) | 8.10(2) | +0.10(2) | [1,20] | 1.4 |
| $^{192}$Hg(1) | 257.7(3) | 4.419(8) | 8.30(10) | 10.12(2) | +0.12(2) | [1,20] | 1.4 |
| $^{193}$Hg(1) | 193.7(3) | 4.607(81) | 9.72(129) | 7.49(17) | −0.01(17) | [15,19] | 3.0 |
| $^{193}$Hg(2) | 254.3(3) | 4.682(26) | 6.31(30) | 10.57(7) | +0.07(7) | [15,19] | 1.0 |
| $^{194}$Hg(1) | 201.2(2) | 4.657(16) | 6.50(23) | 7.95(4) | −0.05(4) | [25,26] | 1.4 |
| $^{194}$Hg(2) | 254.3(1) | 4.413(13) | 8.68(15) | 9.95(3) | −0.05(5) | [25,26] | 1.4 |
| $^{194}$Hg(3) | 262.5(2) | 4.620(32) | 7.07(31) | 10.83(7) | −0.17(7) | [19,26] | 2.0 |
| $^{192}$Pb(1) | 262.6(4) | 4.424(105) | 8.48(133) | 10.37(27) | +0.37(27) | [16] | 2.5 |
| $^{194}$Pb(1) | 169.7(2) | 4.408(24) | 8.17(43) | 6.02(5) | +0.02(5) | [12,13] | 2.5 |
| $^{196}$Pb(1) | 215.0(4) | 4.344(20) | 6.28(27) | 7.94(5) | −0.06(5) | [12,17] | 1.0 |
| $^{198}$Pb(1) | 303.8(4) | 4.265(65) | 5.87(74) | 11.74(17) | −0.26(17) | [17] | 1.0 |
| $^{193}$Tl(1) | 228.1(3) | 4.755(28) | 5.37(39) | 9.46(3) | −0.05(3) | [27] | 1.0 |
| $^{193}$Tl(2) | 248.3(3) | 4.752(32) | 6.16(38) | 10.44(8) | −0.06(8) | [27] | 1.0 |
| $^{194}$Tl(1a) | 268.0(10) | 5.034(65) | 3.61(70) | 12.13(18) | +0.13(18) | [7] | 1.0 |
| $^{194}$Tl(1b) | 209.3(6) | 4.971(49) | 4.53(74) | 8.97(11) | −0.03(11) | [7] | 1.0 |
| $^{194}$Tl(2a) | 240.5(8) | 4.882(47) | 4.14(52) | 10.32(13) | +0.32(13) | [7] | 1.0 |
| $^{194}$Tl(2b) | 220.5(6) | 4.901(46) | 3.91(62) | 9.35(11) | +0.35(11) | [7] | 1.0 |
| $^{194}$Tl(3a) | 226.3(6) | 5.163(47) | 3.44(63) | 10.26(11) | +0.26(11) | [7] | 1.0 |
| $^{194}$Tl(3b) | 245.4(8) | 5.252(58) | 1.55(68) | 11.46(12) | +0.46(13) | [7] | 1.0 |
| $^{195}$Tl(1) | 330.1(7) | 4.589(83) | 7.75(70) | 14.10(26) | −0.40(26) | [18] | 1.0 |
| $^{195}$Tl(2) | 350.7(8) | 4.650(82) | 6.07(64) | 15.22(27) | −0.28(27) | [18] | 1.0 |

[a]Data from the first reference cited were the least-squares input.
[b]Quoted experimental errors are multiplied by $k$.

throughout the text and in tables are based on results with these errors.

Several bands have been observed by more than one experimental group: $^{192}$Hg, $^{193}$Hg, $^{194}$Hg, and $^{194}$Pb. Agreement among the data is good except for one of the bands in $^{193}$Hg. Most unfortunately, the band involved has been labeled by us [19] $^{193}$Hg(1) and by Cullen *et al.* [15] $^{193}$Hg(2). Also, the data of Cullen *et al.* on $^{193}$Hg indicate 4 SD bands, two with almost degenerate energies for a number of transitions. This has led to some confusion. For the present purpose, we use the SD band energies of Ref. [15] since they were determined with knowledge of the nearly degenerate $\gamma$-ray energies. Otherwise, when more than one data set exists, numerical results presented here are based on the measurements we have made. The 214.6-keV transition in SD $^{192}$Hg reported in Ref. [1] has not been confirmed in another study [20]. However, none of the conclusions discussed here for $^{192}$Hg are altered if this transition is excluded from the fit; only fine details of the numerical values are changed. Details are given at appropriate places in the text.

### B. The fitting equations

Least-squares fits were made to these data with two fitting equations. In the first case, the measured $E_\gamma$ of the SD cascade were fit to the equation for the transition energy [Eq. (4)] with $E(I)$ expressed directly by the expansion for $E$ in powers for $I(I+1)$, Eq. (2). In subsequent discussions these least-squares fits will be referred to by Eq. (2) only. The second case is based on the experience (also true here) that an expansion of $I$ in odd powers of $E_\gamma$ converges faster (see, e.g., Refs. [11] and [21]). With the definition $E_\gamma=2\hbar\omega$, and keeping terms to first order, the expansion is

$$\hbar(I+\tfrac{1}{2})=2\alpha\omega+\tfrac{4}{3}\beta\omega^3 \ . \tag{5}$$

In Eq. (5), $I$ refers to the "midpoint" spin of the transition $I+1\rightarrow I-1$. Equation (5) is a phenomenological expression for $I$ in odd powers of $E_\gamma$.

The leading-order term of both fitting equations is just the expression for the transition energy of the quantum rotor:

$$E_\gamma(I+1\rightarrow I-1)=4A(I+\tfrac{1}{2}) \ . \tag{6}$$

Make the substitutions $E_\gamma=2\hbar\omega$ and $2\alpha=\hbar^2/(2A)$ and it is clear that with our definitions the leading-order term relating $E_\gamma$ to $I$ is independent of the choice of fitting equation, as we have already pointed out [22]. The two fitting equations amount to adding higher-order terms to either the left- or right-hand side of the leading-order expression. Our expectation is for a similar description of the data, independent of the fitting-equation choice. [Eq. (5) is often written with the inclusion of a constant term, $i_0$, which represents initial alignment. Discussion of $i_0$ is given in a later section.]

We take the point of view that either approach is valid, and that the SD cascade can be described by either Eq. (2) or (5). Our first choice was the expansion in $E_\gamma/2$ (or $\omega$) since numerous examples have shown that it converges faster. Results for the description of $E$ in terms of an expansion in powers of $I(I+1)$ are also presented, and fitting results obtained with the two approaches compared.

### C. Fits to the $\hbar\omega$ expansion

The nine transitions lowest in energy in each of the 25 SD cascades cited above were fit to Eq. (5) using the code DESCALC [23]. Inverse square weighting was used. We made the reasonable assumption that all SD transitions have multipolarity $L=2$ since, where measurements exist, directional correlations are characteristic of $\Delta I=L=2$. Therefore the fitting equation has three parameters: the two inertial parameters $\alpha$ and $\beta$ and the baseline spin, $I_f$. Fitting results are tabulated in Table I, where the SD bands are identified by nucleus, an arbitrary band label, and the lowest $\gamma$-ray energy included in the fit. The next columns give the fitting parameters $\alpha$, $\beta$, and $I_f$. Uncertainties in the fitting parameters are quoted as either the standard deviation $\sigma$, or $\sigma(\chi^2/\nu)^{1/2}$, which takes into account the scatter in the data. The inertial parameters $\alpha$ and $\beta$ are determined with accuracies of $\sim\frac{1}{4}\%$ and $<10\%$, respectively, while $I_f$ is determined to $\sim 1\%$.

Table I also includes the quantity $\Delta$, which is defined as

$$\Delta=I_f-\text{nearest (half-) integer} \ , \tag{7}$$

depending on the mass identification of the band. This quantity is convenient for comparing the parameter $I_f$ with physical level spin, and for comparing the results of the two fitting equations. The quantity $\Delta$ is illustrated in Fig. 2, where it is ordered according to $N$ and $Z$ of the nucleus: even-even, odd-$A$, and odd-odd.

Insight into the quality and results of the least-squares fits can be illustrated through curves of $\chi^2/\nu$ as a function of $I_f$, and graphical comparison of the experimental dynamic moment of inertia $[\mathcal{J}^{(2)}(\text{exp})]$ with values calculated with the fit parameters $[\mathcal{J}^{(2)}(\text{calc})]$. Results for $^{191}$Hg, $^{192}$Hg, and $^{194}$Hg are presented since these assignments are often discussed. We begin with a discussion of Fig. 3, which illustrates these quantities for the one known SD band in $^{192}$Hg, labeled here $^{192}$Hg(1). The inset in Fig. 3 illustrates $\chi^2/\nu$ vs $I_f$. The smooth curve is a line drawn through discrete values of $\chi^2/\nu$ produced when the least-squares procedure is repeated for incremental values of $I_f$. The curve has a very sharp minimum at $I_f=8.10(2)$. The horizontal dashed line in the inset represents the 95% probability for this value of $\chi^2/\nu$. Numerically, it is clear from the $\chi^2$ curve that Eq. (5) describes these data very well, and that $I_f$ is determined with an uncertainty less than $0.1\hbar$. The field of Fig. 3 compares $\mathcal{J}^{(2)}(\text{exp})$ and $\mathcal{J}^{(2)}(\text{calc})$. Experimental and calculated $E_\gamma$ could be compared, but instead we chose to compare experimental and calculated $\mathcal{J}^{(2)}$, where $\mathcal{J}^{(2)}(\text{exp})$ is given by $\mathcal{J}^{(2)}=4\hbar^2/\Delta E_\gamma$. The equation for $\mathcal{J}^{(2)}$ in terms of the fitting parameters is [28]

$$\mathcal{J}^{(2)}=2\alpha+4\beta\omega^2 \ . \tag{8}$$

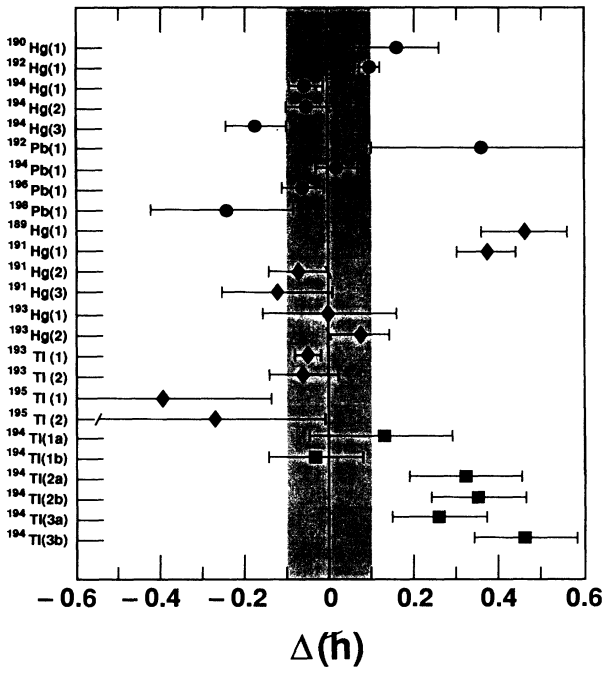


FIG. 2. The values of $\Delta=I_f-$nearest (half-) integer listed in Table I. They were obtained from the least-squares fit of cascade transition energies to the expression for $I$ as a series in odd powers of $\hbar\omega$ ($=E_\gamma/2$), Eq. (5). Values for even-even, odd-$A$, and odd-odd nuclei are labeled by ●, ♦, and ■, respectively. See Table I for references to the data.

The appropriate value of $\hbar\omega$ in Eq. (8) is the average of the transition energies from which $\mathcal{J}^{(2)}$ is computed. A line drawn through the calculated values illustrates $\mathcal{J}^{(2)}$(calc) in Fig. 3. The values were calculated with $I_f$ fixed at $I_f=8$, the nearest quantized spin value consistent with both the least-squares solution and the mass assignment of the SD band. Clearly, experimental and calculated values of $\mathcal{J}^{(2)}$ agree very well, and the fit does not require higher-order terms in Eq. (5) for the range of data included in the least-squares fit. However, $I_f$ cannot yet be identified with level spin because possible alignment at $\omega=0$, $i_0$, has to be considered. This discussion is deferred until Sec. V.

$\mathcal{J}^{(2)}$(calc) produced with parameters obtained from least-squares solutions of Eq. (5) with $I_f$ fixed at $8\pm1$ are also illustrated in Fig. 3. Comparison of these values and $\mathcal{J}^{(2)}$(exp) provides an alternate way of looking at the sensitivity of the solution to $I_f$, and it also conveniently illustrates the frequency range where the expansion of Eq. (5) is valid. The figure shows that not only are the first nine transitions included in the fit well described, but that the same parameters describe at least the first 11 transitions, a range of $22\hbar$. This again stresses the point that SD $^{192}$Hg is an excellent rotor. The kinematic moment of inertia $\mathcal{J}$ calculated from

$$\mathcal{J}=\frac{\hbar^2(2I+1)}{E_\gamma} \tag{9}$$

is also illustrated. Least-squares fit parameters without the 214.6-keV transition are given in Table I; it can be seen from the similarity of the tabulated parameters as well as from Fig. 3 that only fine details of the results depend on this data point.

Results of the least-squares fits to the three bands known in $^{194}$Hg are discussed next with the aid of similar figures. The figure for yrast SD $^{194}$Hg has been presented in Ref. [1], Fig. 1. The band is labeled there and also here as $^{194}$Hg(2). The plot of $\chi^2/\nu$ vs $I_f$ has a sharp minimum at $I_f=9.95(3)$, and experimental and calculated $J^{(2)}$ values compare favorably. This nucleus represents an even better rotor than $^{192}$Hg, in that the cascade is described for 17 transitions or $34\hbar$. Illustrations for the $\gamma$-ray cascades $^{194}$Hg(1) and $^{194}$Hg(3) are presented next in Figs. 4 and 5, respectively. These two cascades are populated with less intensity than $^{194}$Hg(2), and they have been interpreted as signature partners of an excited band in the second minimum [26,19]. The

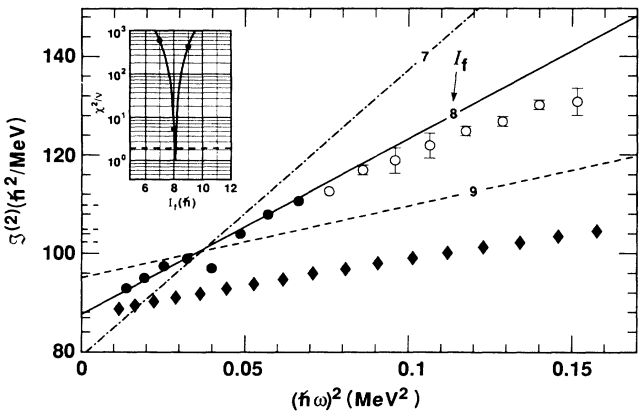


FIG. 3. The quantity $\chi^2/\nu$ vs $I_f$ and $\mathcal{J}^{(2)}$ (○) and $\mathcal{J}^{(1)}$ (♦) for $^{192}$Hg(1). Data points represented by ● correspond to the $\gamma$-ray transitions used in the least-squares fit. The solid line drawn through the data points represents $\mathcal{J}^{(2)}$ calculated with Eq. (8). For comparison, the dot-dashed and dashed lines represent $\mathcal{J}^{(2)}$ calculated with $I_f$(min)$\pm1$.

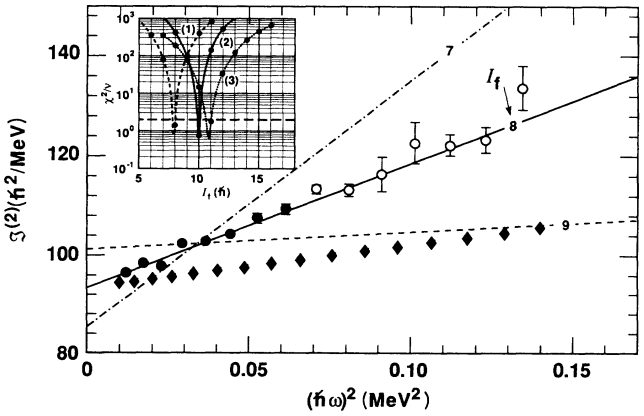


FIG. 4. The quantity $\chi^2/\nu$ vs $I_f$ for $^{194}$Hg(1,2,3) and $\mathcal{J}^{(2)}$ (○) and $\mathcal{J}^{(1)}$ (♦) for $^{194}$Hg(1). See also Fig. 3

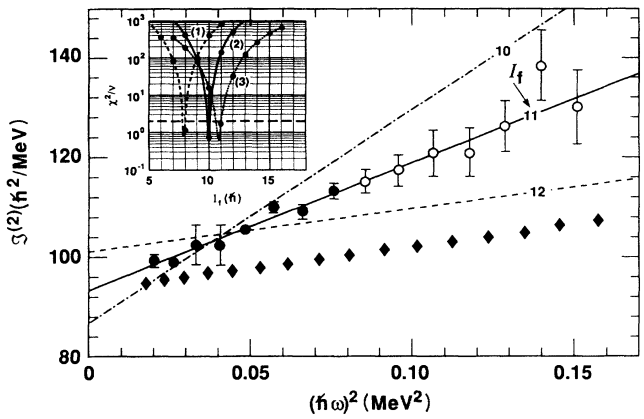


FIG. 5. The quantity $\chi^2/\nu$ vs $I_f$ for $^{194}$Hg(1,2,3) and $\mathcal{J}^{(2)}$ (○) and $\mathcal{J}^{(1)}$ (◆) for $^{194}$Hg(3). See also Fig. 3.

$\chi^2/\nu$ curves reach clear, well-defined, sharp minima for both signature partners: $I_f$ is determined very well and comparison between $\mathcal{J}^{(2)}$(exp) and $\mathcal{J}^{(2)}$(calc) is very good.

Illustration of the least-squares fitting concludes with Fig. 2 in Ref. [4], which presented fitting results for the three SD cascades reported in $^{191}$Hg. Values of $\chi^2/\nu$ vs $I_f$ for all three cascades are given in the inset. The two signature partner SD bands in $^{191}$Hg (labeled 2 and 3) have minima near half-integer values, but the band $^{191}$Hg(1) offers the first surprise, with $I_f$(min)=14.87(7), closer to integer than half-integer, although the mass assignment requires a half-integer value. Experimental and calculated $\mathcal{J}^{(2)}$ for $^{191}$Hg(1) are illustrated in the field of the figure. The fitting was repeated, including only the five transitions lowest in energy, with the result $I_f$=15.34(22). Thus, the low-frequency data suggest $\frac{31}{2}$ rather than $\frac{29}{2}$ as the nearest half-odd integer value in this case. Cranking-model calculations can provide some insight into this behavior, and we discuss this point in Sec. V.

The figures presented along with the data of Table I show the selectivity of the fits towards an (half-) integer value of $I_f$, depending on the $A,Z$ of the nucleus. The values of $I_f$ modulo (half) integer for the entire data set are listed in Table II, fifth column, taking the mass assignment into account when required. The two values of $I_f$ nearest the minimum are listed in those cases where

TABLE II. Parameters from the least-squares fit of transitions 1–9 (beginning with the lowest energy) to Eq. (5) with $I_f$ fixed at the nearest (half-) integer. Data are arranged according to whether or not a signature band has been observed. The parameter $\alpha$ corresponds to $\frac{1}{2}$ the moment of inertia. See Table I for references. Spin values marked by an asterisk are the (half-) integer value nearest the minimum of the fitting parameter $I_f$ listed in Table I.

| $^A$Z | $E_\gamma$ (keV) | $10^2\alpha$ ($\hbar^2$/keV) | $10^8\beta$ ($\hbar^2$/keV$^3$) | $I_f$ ($\hbar$) |
|---|---|---|---|---|
| | | Cascades without signature partner | | |
| $^{189}$Hg(1) | 366.0(4) | 4.541(6) | 4.26(14) | ($\frac{29}{2}$*, $\frac{31}{2}$) |
| $^{190}$Hg(1) | 360.0(2) | 4.129(3) | 8.51(6) | 14 |
| $^{191}$Hg(1) | 350.6(1) | 4.444(5) | 6.48(10) | ($\frac{29}{2}$*, $\frac{31}{2}$) |
| $^{192}$Hg(1) | 214.6(3) | 4.366(2) | 9.03(8) | 8 |
| $^{192}$Hg(1) | 257.7(3) | 4.369(3) | 8.90(9) | 10 |
| $^{194}$Hg(2) | 254.3(1) | 4.430(1) | 8.49(4) | 10 |
| $^{192}$Pb(1) | 262.6(4) | 4.281(13) | 10.2(5) | 10*,11 |
| $^{194}$Pb(1) | 169.7(2) | 4.398(4) | 8.33(16) | 6 |
| $^{196}$Pb(1) | 215.0(4) | 4.369(2) | 5.95(11) | 8 |
| $^{198}$Pb(1) | 303.8(4) | 4.361(7) | 4.83(21) | 12 |
| | | Cascades with signature partner | | |
| $^{191}$Hg(2) | 292.0(2) | 4.713(3) | 5.21(8) | $\frac{25}{2}$ |
| $^{191}$Hg(3) | 311.8(4) | 4.709(4) | 6.14(9) | $\frac{27}{2}$ |
| $^{193}$Hg(1) | 193.7(3) | 4.610(13) | 9.68(45) | $\frac{15}{2}$ |
| $^{193}$Hg(2) | 254.3(3) | 4.653(3) | 6.63(10) | $\frac{21}{2}$ |
| $^{194}$Hg(1) | 201.2(2) | 4.677(2) | 6.23(8) | 8 |
| $^{194}$Hg(3) | 262.5(2) | 4.682(4) | 6.38(11) | 11 |
| $^{193}$Tl(1) | 228.1(3) | 4.777(5) | 5.07(11) | $\frac{19}{2}$ |
| $^{193}$Tl(2) | 248.3(3) | 4.773(4) | 5.92(11) | $\frac{21}{2}$ |
| $^{194}$Tl(1a) | 268.0(10) | 4.988(7) | 4.09(19) | 12 |
| $^{194}$Tl(1b) | 209.3(6) | 4.984(7) | 4.37(26) | 9 |
| $^{194}$Tl(2a) | 240.5(8) | 4.766(8) | 5.35(19) | (10*,11) |
| $^{194}$Tl(2b) | 220.5(6) | 4.756(11) | 5.77(31) | (9*,10) |
| $^{194}$Tl(3a) | 226.3(6) | 5.058(8) | 4.77(23) | (10*,11) |
| $^{194}$Tl(3b) | 245.4(8) | 5.054(10) | 4.37(34) | (11*,12) |
| $^{195}$Tl(1) | 330.1(7) | 4.556(8) | 8.02(17) | ($\frac{29}{2}$) |
| $^{195}$Tl(2) | 350.7(8) | 4.583(8) | 6.58(17) | ($\frac{31}{3}$) |

the minimum falls at a value that is unexpected from the mass assignment.

The entire data set was fit again with $I_f$ fixed at the nearest (half-) integer value. Values of $\alpha$ and $\beta$ result with substantially reduced errors as expected: they are listed in Table II. Discussion of this table is given in Sec. V.

### D. Fits to $\mathcal{J}^{(2)}$

Least-squares fits can be made using Eq. (8), the expression for $\mathcal{J}^{(2)}$. The fitting parameters in this case are $\alpha$ and $\beta$, and $\mathcal{J}^{(2)}$ is obtained from the experimental quantities, $E_\gamma$. Level spin is obtained by substitution in Eq. (5). Draper *et al.* [28] have presented details of the power-series expansion for $\mathcal{J}^{(2)}$ in terms of $\omega$. The quantity $\mathcal{J}^{(2)}$ is obtained from the difference in adjacent transitions in the cascade, and this introduces correlations into the fit. Fitting done with Eq. (5) or Eq. (2), on the other hand, uses the experimental $E_\gamma$ directly. A sample of numerical examples of least-squares fittings done with Eqs. (5) and (8) are listed in Table III. [In subsequent discussions, these least-squares fits and the resulting parameters will be referred to by Eq. (8).] Consistent parameter values are obtained with both procedures, and in particular $I_f$ does not change much. The least-squares estimate of the parameter errors is overestimated with Eq. (8) because errors are compounded in quadrature when the input values of $\mathcal{J}^{(2)}$ are computed. A better estimate of the error is obtained when the least-squares fitting is done to Eq. (5).

### E. A term in $\omega^2$?

Empirical tests were made to see if a better fit to the data or a different result could be obtained by including a term in $\omega^2$ in Eq. (5). Therefore, the least-squares fitting was repeated with the term $x\omega^2$ added to Eq. (5) for the yrast cascades of $^{192}$Hg and $^{194}$Hg, both excellent examples of rotational cascades. The fits were done with the power-series expansion for $I$ terminated at either quadratic or cubic powers of $\omega$. The results, listed in Table IV, show that a description in terms of an expansion which only includes terms in $\omega$ and $\omega^2$ is not adequate for these data sets, and more generally that the $\omega^2$ term is not needed, as one might expect if identification of $\omega$ with an angular velocity is made.

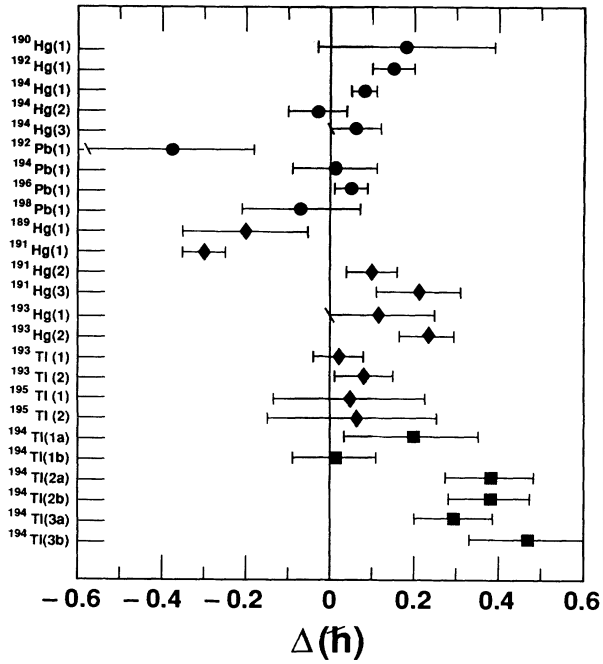


FIG. 6. The quantity $\Delta=I_f-$nearest (half-) integer listed in Table V. The value of $I_f$ was obtained from the least-squares fit of cascade transition energies to $E(I+2\rightarrow I)=E(I+2)-E(I)$, with $E(I)$ expressed as a power series in $I(I+1)$, Eq. (2). Values for even-even, odd-$A$, and odd-odd nuclei are labeled by ●, ♦, and ■, respectively. See Table I for references to the data.

### F. Fits using the expansion of $E$ in powers of $I(I+1)$

Least-squares fits of the same data were made to the equation for $E_\gamma$, $E_\gamma=E(I+2)-E(I)$, [Eq. (4)], with $E(I)$ expressed as a series in powers of $I(I+1)$, $E(I)=AI(I+1)+BI^2(I+1)^2+CI^3(I+1)^3$ [Eq. (2)].

TABLE III. Comparison of parameters from the least-squares fit of transitions 1–9 (beginning with the lowest energy) of SD cascades $^{192}$Hg and $^{194}$Hg(1,2,3) to Eq. (5) and to Eq. (8). Rows labeled by $\omega$ refer to fits to Eq. (5), $\hbar(I+\frac{1}{2})=2\alpha\omega+\frac{4}{3}\beta\omega^3$, and rows labeled by $\mathcal{J}^{(2)}$ refer to fits to Eq. (8), $\mathcal{J}^{(2)}=2\alpha+4\beta\omega^2$. See also the caption and references for Table I.

| Fit | $^A$Z | $E_\gamma$ (keV) | $10^2\alpha$ ($\hbar^2$/keV) | $10^8\beta$ ($\hbar^2$/keV$^3$) | $I_f$ ($\hbar$) | $\Delta$ ($\hbar$) |
|---|---|---|---|---|---|---|
| $\omega$ | $^{192}$Hg(1) | 214.6(3) | 4.410(8) | 8.44(11) | 8.10(2) | +0.02(2) |
| $\mathcal{J}^{(2)}$ | $^{192}$Hg(1) | 214.6(3) | 4.413(17) | 8.48(26) | 8.12(3) | +0.12(3) |
| $\omega$ | $^{194}$Hg(1) | 201.2(2) | 4.657(16) | 6.50(23) | 7.95(4) | −0.05(4) |
| $\mathcal{J}^{(2)}$ | $^{194}$Hg(1) | 201.2(2) | 4.651(40) | 6.57(55) | 7.97(7) | −0.03(7) |
| $\omega$ | $^{194}$Hg(2) | 254.3(1) | 4.413(13) | 8.68(15) | 9.95(3) | −0.05(3) |
| $\mathcal{J}^{(2)}$ | $^{194}$Hg(2) | 254.3(1) | 4.416(23) | 8.58(27) | 9.98(5) | −0.02(5) |
| $\omega$ | $^{194}$Hg(3) | 262.5(2) | 4.620(32) | 7.07(31) | 10.83(7) | −0.17(7) |
| $\mathcal{J}^{(2)}$ | $^{194}$Hg(3) | 262.5(2) | 4.625(56) | 6.99(61) | 10.84(13) | −0.16(13) |

TABLE IV. Fitting parameters calculated when a test quadratic term is added to Eq. (5), $\hbar(I+\frac{1}{2})=2\alpha\omega+\frac{4}{3}\beta\omega^3+x\omega^2$. The data are transitions 1–9 (beginning with the lowest energy) of the yrast SD cascades in $^{192,194}$Hg. The power-series expansion is terminated at either quadratic or cubic powers of $\omega$, and $x$ is the amplitude of the test quadratic term. See Table I for references.

| $^AZ$ | $E_\gamma$ (keV) | $10^2\alpha$ ($\hbar^2$/keV) | $10^8\beta$ ($\hbar^3$/keV$^3$) | $10^6x$ ($\hbar^2$keV$^2$) | $I_f$ ($\hbar$) | $\chi^2/\nu$ |
|---|---|---|---|---|---|---|
| $^{192}$Hg(1) | 214.6(3) | 4.410(8) | 8.44(11) | | 8.10(2) | 1.20 |
| $^{192}$Hg(1) | 214.6(3) | 4.428(138) | 8.69(195) | 01.92(1488) | 8.15(17) | 1.44 |
| $^{192}$Hg(1) | 214.6(3) | 4.428(138) | | 63.18(184) | 7.40(6) | 6.00 |
| $^{194}$Hg(2) | 254.3(1) | 4.412(13) | 8.67(15) | | 9.98(3) | 0.76 |
| $^{194}$Hg(2) | 254.3(1) | 4.296(171) | 7.24(190) | 11.71(1560) | 9.83(20) | 0.82 |
| $^{194}$Hg(2) | 254.3(1) | 3.711(41) | | 70.78(200) | 9.08(8) | 2.72 |

The fitting parameters are $A$, $B$, $C$, and $I_f$. As in the fits to Eq. (5), the nine cascade transitions lowest in energy were used in the fit, with quoted $\gamma$-ray energy errors multiplied by the factors $k$ given in Table I. Excellent fits were obtained, and results are summarized by the entries in Table V. The bands are labeled as in Table I, that is, by the band label given in the original reference, and the lowest-energy $\gamma$ ray included in the fit. Entries include the fitting parameters $A$, $B$, $C$, and $I_f$, and $\Delta$. The parameter $C$ is given only in the few cases (4 out of 25) where the fit required a second-order correction term, as measured by $\chi^2/\nu$. The (half) integer nearest the least-squares fitting parameter $I_f$ for these fits is the same as for the fits to Eq. (5) for 22 of the 25 bands, and one unit greater for the SD bands labeled $^{189}$Hg(1), $^{191}$Hg(1), and $^{192}$Pb. The values of $\Delta$ are plotted in Fig. 6 and it can be seen that these fits also suggest $I_f$ as (half) integer for bands in even-even and odd-$A$ nuclei. Comparisons of data and quantities calculated with the least-squares estimate are not given here because extensive comparisons obtained with the least-squares estimates resulting from the fit to Eq. (5) have already been given in Sec. III C.

TABLE V. Parameters from the least-squares fit of transitions 1–9 in the SD cascade (beginning with the lowest energy) to Eqs. (4) and (2). Here, $E(I)$ is represented as a power series in $I(I+1)$, $E(I)=AI(I+1)+B[I(I+1)]^2+\cdots$. All transitions are taken as $\Delta I=L=2$, and the least-squares parameter $I_f$ corresponds to the baseline spin of the SD cascade. See Table I for references.

| $^AZ$ | $E_\gamma$ (keV) | $A$ (keV/$\hbar^2$) | $10^4B$ (keV/$\hbar^4$) | $10^8C$ (keV/$\hbar^6$) | $I_f$ ($\hbar$) | $\Delta$ ($\hbar$) |
|---|---|---|---|---|---|---|
| $^{189}$Hg(1) | 366.0(4) | 5.553(52) | −1.87(18) | | 15.30(15) | −0.20(15) |
| $^{190}$Hg(1) | 360.0(2) | 5.966(98) | −4.78(70) | 7.7(24) | 14.18(21) | +0.18(21) |
| $^{191}$Hg(1) | 350.6(1) | 5.336(17) | −1.61(5) | | 15.20(5) | −0.30(5) |
| $^{191}$Hg(2) | 292.0(2) | 5.246(23) | −1.59(9) | | 12.60(6) | +0.10(6) |
| $^{191}$Hg(3) | 311.8(4) | 5.205(32) | −1.68(10) | | 13.71(10) | +0.21(10) |
| $^{192}$Hg(1) | 214.6(3) | 5.639(30) | −4.07(35) | 6.7(20) | 8.15(5) | +0.15(5) |
| $^{192}$Hg(1) | 257.7(3) | 5.647(21) | −4.17(23) | 7.3(11) | 10.13(5) | +0.13(5) |
| $^{193}$Hg(1) | 193.7(3) | 5.337(56) | −2.97(33) | | 7.62(12) | +0.12(12) |
| $^{193}$Hg(2) | 254.3(3) | 5.257(22) | −1.86(9) | | 10.73(6) | +0.23(6) |
| $^{194}$Hg(1) | 201.2(2) | 5.308(14) | −2.07(8) | | 8.08(3) | +0.08(3) |
| $^{194}$Hg(2) | 254.3(1) | 5.661(37) | −4.40(36) | 8.0(17) | 9.97(7) | −0.03(7) |
| $^{194}$Hg(3) | 262.5(2) | 5.290(22) | −2.02(9) | | 11.06(6) | +0.06(6) |
| $^{192}$Pb(1) | 262.6(10) | 5.498(88) | −2.72(44) | | 10.62(21) | −0.38(21) |
| $^{194}$Pb(1) | 169.7(2) | 5.681(74) | −4.51(112) | 10.0(80) | 6.01(10) | +0.01(10) |
| $^{196}$Pb(1) | 215.0(4) | 5.678(20) | −2.55(11) | | 8.05(4) | +0.05(04) |
| $^{198}$Pb(1) | 303.8(4) | 5.749(63) | −2.41(32) | | 11.93(14) | −0.07(14) |
| $^{193}$Tl(1) | 228.1(3) | 5.214(24) | −1.66(12) | | 9.52(6) | +0.02(6) |
| $^{193}$Tl(2) | 248.3(3) | 5.187(27) | −1.75(12) | | 10.58(7) | +0.08(7) |
| $^{194}$Tl(1a) | 268.0(10) | 4.934(54) | −0.93(19) | | 12.20(16) | +0.20(16) |
| $^{194}$Tl(1b) | 209.3(6) | 5.005(42) | −1.26(21) | | 9.01(10) | +0.01(10) |
| $^{194}$Tl(2a) | 240.5(8) | 5.089(41) | −1.20(16) | | 10.38(11) | +0.38(11) |
| $^{194}$Tl(2b) | 220.5(6) | 5.079(40) | −1.16(18) | | 9.38(10) | +0.38(10) |
| $^{194}$Tl(3a) | 226.3(6) | 4.826(38) | −0.85(16) | | 10.29(10) | +0.29(10) |
| $^{194}$Tl(3b) | 245.4(8) | 4.754(49) | −0.39(17) | | 11.47(14) | +0.47(14) |
| $^{195}$Tl(1) | 330.1(7) | 5.247(58) | −1.96(18) | | 14.55(18) | +0.05(18) |
| $^{195}$Tl(2) | 350.7(8) | 5.227(59) | −1.60(17) | | 15.56(20) | +0.06(20) |

## IV. DISCUSSION OF THE FITTING EQUATIONS

Topics in this section include the convergence of the fitting equations as manifested by the number of higher-order terms required to produce a value of $\chi^2/\nu \sim 1$, the departure of $\Delta$ from (half-) integer values of $I_f$, and the estimate of $I_f$ produced from the two transitions lowest in energy.

### A. Convergence of the fits

Previous work has suggested that the radius of convergence is smaller for Eq. (5) than for Eq. (2). Most of the results presented here were done with nine points included in the data set. The SD cascades $^{190}$Hg(1), $^{192}$Hg(1), $^{194}$Hg(2), and $^{194}$Pb(1) required the second-order term $CI^3(I+1)^3$ in the $I(I+1)$ expansion for the least-squares fit to achieve $\chi^2/\nu \sim 1$. On the other hand, a satisfactory fit by Eq. (5) never required a second-order term. As examples, details of the fitting parameters calculated with and without the second-order term for the SD bands in $^{192}$Hg and $^{194}$Hg are summarized in Table VI.

While nothing here is surprising in view of past results, this is the first time that so many data points could be included in the fit and that the coefficient $C$ could be determined accurately. We conclude that the expansion of $I$ in terms of $\omega$ converges somewhat better than the expansion of energy in terms of $I(I+1)$ for the data set used here.

### B. Departure of $\Delta$ from 0

Two fitting equations have been applied to 25 SD bands, Eqs. (2) and (5). The least-squares parameters $I_f$, the baseline spin of the SD cascade, and $\Delta$, $I_f -$ the nearest (half-) integer, are summarized for the 25 SD bands and the two fitting equations in Tables I and V, respectively. The (half) integer nearest the parameter $I_f$ is the same in 22 of the 25 cases. This quantity shifts up one unit in the three cases $^{192}$Pb and $^{189,191}$Hg(1) when the fitting equation is Eq. (2). Values of $\Delta$ are plotted in Figs. 2 and 6. The weighted mean $\bar{\Delta}$ and the rms deviation $\Delta_{\rm rms}$ of $\Delta$ for the even-even, odd-$A$, and odd-odd nuclei, and also for the aggregate are listed in Table VII for both fitting equations. The values of $\Delta_{\rm rms}$ increase for the even-even, odd-$A$, and odd-odd nuclei, in that order. Both $\bar{\Delta}$ and $\Delta_{\rm rms}$ are less than $0.1\hbar$ for the even-even nuclei. Figure 2 shows that $\Delta$ falls within $0\pm0.1\hbar$ for 18 of the 25 bands considered, and in Fig. 6 the corresponding statistic is 17 of 25 bands. The quantity $\Delta$ is closer to 0 for $^{195}$Tl(1,2) in Fig. 6 [Eq. (2)]. The distinction between the two fitting equations does not appear to be significant if the value of $\Delta_{\rm rms}$ for the even-even nuclei is used as a criterion. In thinking about these data, recall that the bands in even-even nuclei tend to be populated more intensely than the other nuclei, and also that the cascade proceeds to lower spin.

### C. Effect of reduction of the number of points in fit

Suggestions have been made [8–10] that the parameter $I_f$ is very sensitive to the number of points included in the fit, and that results are very different if the data are restricted to a few low-energy transitions. Wu, Feng, and Guidry [8,9] suggest in particular that $I_f$ is not determined to better than $\pm2\hbar$. Apart from the question of adequate statistics, this suggestion implies different behavior of the frequency dependent alignment at the low-, middle-, and high-frequency range included in the fits described here. Studies were made of the effect on the fitting parameters when the data set was restricted to the five (rather than nine) transitions lowest in energy. Table VIII lists the fit parameters obtained for 10 Hg SD cascades. Our conclusion from a study of Table VIII is that when the number of transitions included in the fit is reduced from nine to five, the main effect is reduced accuracy in the determination of $\alpha$, $\beta$, and $I_f$. [The case of $^{191}$Hg(1), where $I_f$ changes by one unit, is the sole exception.]

The extreme case is obtained when the data set is restricted to the two transitions lowest in energy, and $I_f$ estimated using the relationship $\Delta E_\gamma/E_\gamma = \Delta I/I$. Results are listed in Table IX, where the parameter $I_f$ obtained in the fit with nine data points to Eqs. (5) and (2) is listed again for comparison. There is no case where $I_f$ differs by as much as 1 unit from the values listed in Table I. The values of $\bar{\Delta}$ and $\Delta_{\rm rms}$ are $0.05(3)\hbar$ and $0.14(2)\hbar$, respectively, for the two transition estimates. Three estimates of the fitting parameter $I_f$ are given for 25 SD

TABLE VI. Parameters and fitting details of the least-squares fit of transitions 1–9 (beginning with the lowest energy) to the SD cascades in $^{192,194}$Hg to Eqs. (2) and (4). The power-series expansion for $E$, $E(I)=AI(I+1)+\cdots$, is terminated alternately at quadratic and cubic powers of $I(I+1)$. See Table I for references.

| $^AZ$ | $E_\gamma$ (keV) | $A$ (keV/$\hbar^2$) | $10^4B$ (keV/$\hbar^2$) | $10^8C$ (keV/$\hbar^2$) | $I_f$ ($\hbar$) | $\nu$ | $\chi^2/\nu$ |
|---|---|---|---|---|---|---|---|
| $^{192}$Hg(1) | 214.6(3) | 5.538(12) | 2.87(7) | | 8.31(3) | 6 | 3.91 |
| $^{192}$Hg(1) | 214.6(3) | 5.639(30) | 4.07(35) | 6.7(20) | 8.15(5) | 5 | 1.42 |
| $^{194}$Hg(1) | 201.2(2) | 5.308(14) | 2.07(8) | | 8.08(3) | 6 | $8.54\times10^{-1}$ |
| $^{194}$Hg(1) | 201.2(2) | 5.339(45) | 2.43(51) | 2.0(28) | 8.03(8) | 5 | $9.22\times10^{-1}$ |
| $^{194}$Hg(2) | 254.3(1) | 5.487(22) | 2.68(10) | | 10.29(5) | 6 | 4.26 |
| $^{194}$Hg(2) | 254.3(1) | 5.661(37) | 4.40(36) | 8.0(17) | 9.97(7) | 5 | 5.86 |
| $^{194}$Hg(3) | 262.5(2) | 5.290(22) | 2.02(9) | | 11.06(6) | 6 | $9.45\times10^{-1}$ |
| $^{194}$Hg(3) | 262.5(2) | 5.393(84) | 2.92(73) | 3.8(31) | 10.86(17) | 5 | $8.25\times10^{-1}$ |

TABLE VII. Mean values of Δ from the values listed in Tables I and V. Rows labeled by $\omega$ refer to fits to Eq. (5) (Table I), and rows labeled by $I(I+1)$ refers to fits to Eq. (2) (Table V). The (half-) integer closest to the least-squares fitting parameter $I_f$ is one unit greater for the SD bands labeled $^{189}$Hg(1), $^{191}$Hg(1), and $^{192}$Pb for the fitting $I(I+1)$ compared to $\omega$. See Table I for references.

| Fit | even-even | odd-$A$ | odd-odd | aggregate |
|---|---|---|---|---|
| | | $\bar{\Delta}$ | | |
| $\omega$ | 0.034(31) | −0.009(83) | 0.247(73) | 0.041(27) |
| $I(I+1)$ | 0.065(22) | 0.037(53) | 0.274(70) | 0.070(30) |
| | | $\Delta_{\rm rms}$ | | |
| $\omega$ | 0.085(15) | 0.189(54) | 0.260(64) | 0.102(19) |
| $I(I+1)$ | 0.078(16) | 0.137(29) | 0.274(70) | 0.120(19) |

bands in Table IX. Comparing values of the quantity $I_f-$ the nearest (half-) integer given in the third, fifth, and seventh columns shows three cases where the two-transition (estimate column 7) is different if the comparison is made to the fitting results of Eq. (5) (third column), and one case if the comparison is made with the fitting results of Eq. (2) (fifth column). It seems that (i) a good estimate of SD band spin can be obtained from the first two low-energy transitions of the band for these data, and (ii) $I_f$ remains the same with very few exceptions when the fitting is done to the two, five, or nine data points lowest in energy, except for $^{191}$Hg(1). Wu *et al.* [8,9] draw a different conclusion.

Lastly, it is useful to point out again that these are difficult experiments. The SD bands depopulate at low spin, and the lowest-energy transitions observed may not have the full intensity of the band. Background, always high, may also be higher in the low-energy ($E_\gamma \sim 200$ keV) portion of the spectrum than at a higher energy (400 keV). It is possible that the lowest-energy point may not belong to the band at all, or that its energy (or the energy of a nearby transition) is not determined particularly well. Prudence suggests that the fit include more than the minimum number of points necessary to obtain an answer, and that the $\chi^2$ test (or some other test of significance) be employed to determine the quality of the fit.

## V. DISCUSSION OF THE FITTING PARAMETERS

### A. Identification of $I_f$ with spin

We will identify $I_f$ with level spin for all the SD bands of Table I with a value of Δ that includes $\Delta = 0 \pm 0.1$ for

TABLE VIII. Comparison of parameters from the least-squares fit of transitions 1–5 and transitions 1–9 (beginning with the lowest energy) to Eq. (5), $\hbar(I+\frac{1}{2}) = 2\alpha + \frac{4}{3}\beta\omega^3$. Transitions are assumed to be stretched quadrupole, and the fitting parameter $I_f$ is the baseline spin of the cascade. See Table I for references.

| No. | $^A$Z | $E_\gamma$ (keV) | $10^2\alpha$ ($\hbar^2$/keV) | $10^8\beta$ ($\hbar^2$/keV$^3$) | $I_f$ ($\hbar$) | Δ ($\hbar$) |
|---|---|---|---|---|---|---|
| 5 | $^{189}$Hg(1) | 366.0(4) | 4.327(180) | 6.06(183) | 14.83(52) | +0.33(52) |
| 9 | $^{189}$Hg(1) | 366.0(4) | 4.373(63) | 5.58(51) | 14.96(10) | +0.46(10) |
| 5 | $^{191}$Hg(1) | 350.6(1) | 4.728(78) | 3.75(85) | 15.34(22) | −0.16(22) |
| 9 | $^{191}$Hg(1) | 350.6(1) | 4.558(22) | 5.62(17) | 14.87(7) | +0.37(7) |
| 5 | $^{191}$Hg(2) | 292.0(2) | 4.597(67) | 6.77(89) | 12.21(17) | −0.29(17) |
| 9 | $^{191}$Hg(2) | 292.0(2) | 4.689(26) | 5.45(59) | 12.43(7) | −0.07(7) |
| 5 | $^{191}$Hg(3) | 311.8(4) | 4.760(150) | 5.27(175) | 13.61(40) | +0.11(40) |
| 9 | $^{191}$Hg(3) | 311.8(4) | 4.662(42) | 6.45(35) | 13.38(13) | −0.12(13) |
| 5 | $^{192}$Hg(1) | 214.6(3) | 4.443(25) | 7.76(50) | 8.17(5) | +0.17(5) |
| 9 | $^{192}$Hg(1) | 214.6(3) | 4.410(8) | 8.44(11) | 8.10(2) | +0.10(2) |
| 5 | $^{193}$Hg(1) | 193.7(3) | 4.841(216) | 4.41(558) | 7.92(38) | +0.42(38) |
| 9 | $^{193}$Hg(1) | 193.7(3) | 4.607(81) | 9.72(129) | 7.49(17) | −0.01(17) |
| 5 | $^{193}$Hg(2) | 254.3(3) | 4.710(88) | 5.91(154) | 10.64(14) | +0.14(14) |
| 9 | $^{193}$Hg(2) | 254.3(3) | 4.682(26) | 6.31(30) | 10.57(7) | +0.07(7) |
| 5 | $^{194}$Hg(1) | 201.2(2) | 4.671(64) | 6.15(148) | 8.01(12) | +0.01(12) |
| 9 | $^{194}$Hg(1) | 201.2(2) | 4.657(16) | 6.50(23) | 7.95(4) | −0.05(4) |
| 5 | $^{194}$Hg(2) | 254.3(1) | 4.404(43) | 8.78(71) | 9.96(10) | −0.04(10) |
| 9 | $^{194}$Hg(2) | 254.3(1) | 4.413(13) | 8.68(15) | 9.95(3) | −0.05(5) |
| 5 | $^{194}$Hg(3) | 262.5(2) | 4.649(81) | 6.61(124) | 10.90(19) | −0.10(19) |
| 9 | $^{194}$Hg(3) | 262.5(2) | 4.620(32) | 7.07(31) | 10.83(7) | −0.17(7) |

TABLE IX. The parameter $I_f$ (in $\hbar$) and the associated $\Delta$ from the least-squares fit of transitions 1–9 (beginning with the lowest energy) to Eq. (5) ($\omega$), to Eqs. (2) and (4) $[I(I+1)]$, and the two-transition estimate $[\Delta I(E_\gamma/\Delta E_\gamma)-2]$. See Table I for references.

| | | $\omega$ | | $I(I+1)$ | | $\Delta I(E_\gamma/\Delta E_\gamma)-2$ | |
|---|---|---|---|---|---|---|---|
| $^{A}Z$ | $E_\gamma$ (keV) | $I_f$ | $\Delta$ | $I_f$ | $\Delta$ | $I_f$ | $\Delta$ |
| $^{189}$Hg(1) | 366.0(4) | 14.96(10) | +0.46(10) | 15.30(15) | −0.20(15) | 15.6(2) | +1.1(2) |
| $^{190}$Hg(1) | 360.0(2) | 14.16(10) | +0.16(10) | 14.18(21) | +0.18(21) | 14.9(1) | +0.09(1) |
| $^{191}$Hg(1) | 350.6(1) | 14.87(7) | +0.37(7) | 15.20(5) | −0.30(5) | 15.6(1) | +1.1(1) |
| $^{191}$Hg(2) | 292.0(2) | 12.43(7) | −0.07(7) | 12.60(6) | +0.10(6) | 12.3(1) | −0.2(1) |
| $^{191}$Hg(3) | 311.8(4) | 13.38(13) | −0.12(13) | 13.71(10) | +0.21(10) | 13.7(3) | +0.2(3) |
| $^{192}$Hg(1) | 214.6(3) | 8.10(2) | +0.10(2) | 8.15(5) | +0.15(5) | 8.0(1) | +0.0(1) |
| $^{193}$Hg(1) | 193.7(3) | 7.49(17) | −0.01(17) | 7.62(12) | +0.12(12) | 7.8(3) | +0.3(3) |
| $^{193}$Hg(2) | 254.3(3) | 10.57(7) | +0.07(7) | 10.73(6) | −0.23(6) | 10.5(1) | +0.0(1) |
| $^{194}$Hg(1) | 201.2(2) | 7.95(4) | −0.05(4) | 8.08(3) | +0.08(3) | 7.7(1) | −0.3(1) |
| $^{194}$Hg(2) | 254.3(1) | 9.95(3) | −0.05(5) | 9.97(7) | −0.03(7) | 10.1(1) | +0.1(1) |
| $^{194}$Hg(3) | 262.5(2) | 10.83(7) | −0.17(7) | 11.06(6) | +0.06(6) | 11.1(1) | +0.1(1) |
| $^{192}$Pb(1) | 262.6(4) | 10.37(27) | +0.37(27) | 10.62(21) | −0.38(21) | 10.7(2) | +0.2(2) |
| $^{194}$Pb(1) | 169.7(2) | 6.02(5) | +0.02(5) | 6.01(10) | +0.01(10) | 5.9(1) | −0.1(1) |
| $^{196}$Pb(1) | 215.0(4) | 7.94(5) | −0.06(5) | 8.05(4) | +0.05(4) | 7.8(1) | −0.2(1) |
| $^{198}$Pb(1) | 303.8(4) | 11.74(17) | −0.26(17) | 11.93(14) | −0.07(14) | 11.7(2) | −0.3(2) |
| $^{193}$Tl(1) | 228.1(3) | 9.46(3) | −0.05(3) | 9.52(6) | +0.02(6) | 9.3(1) | −0.2(1) |
| $^{193}$Tl(2) | 248.3(3) | 10.44(8) | −0.06(8) | 10.58(7) | +0.08(7) | 10.6(1) | +0.1(1) |
| $^{194}$Tl(1a) | 268.0(10) | 12.13(18) | +0.13(18) | 12.20(16) | +0.20(16) | 11.7(2) | −0.3(2) |
| $^{194}$Tl(1b) | 209.3(6) | 8.97(11) | −0.03(11) | 9.01(10) | +0.01(10) | 8.7(2) | −0.3(2) |
| $^{194}$Tl(2a) | 240.5(8) | 10.32(13) | +0.32(13) | 10.38(11) | +0.38(11) | 10.2(3) | +0.2(3) |
| $^{194}$Tl(2b) | 220.5(6) | 9.35(11) | +0.35(11) | 9.38(10) | +0.38(10) | 9.3(2) | +0.3(2) |
| $^{194}$Tl(3a) | 226.3(6) | 10.26(11) | +0.26(11) | 10.29(10) | +0.29(10) | 9.8(3) | −0.2(3) |
| $^{194}$Tl(3b) | 245.4(8) | 11.46(12) | +0.46(13) | 11.47(14) | +0.47(14) | 10.8(3) | −0.2(3) |
| $^{195}$Tl(1) | 330.1(7) | 14.10(26) | −0.40(26) | 14.55(18) | +0.05(18) | 14.5(5) | +0.0(5) |
| $^{195}$Tl(2) | 350.7(8) | 15.22(27) | −0.28(27) | 15.56(20) | +0.06(20) | 15.9(5) | +0.4(5) |

the reasons given below, and suggest that we have identified the most likely spin range for the other nuclei. The evidence is most compelling for the even-even nuclei, suggestive for the odd-$A$ nuclei, and less compelling for the single odd-odd nucleus studied in the $A=194$ mass region.

The following discussion emphasizes the fitting results obtained with Eq. (5) because of its slightly better convergence; however, if the fitting results of Eq. (2) were used the general conclusions would be the same. Results summarized in Table I and illustrated (in part) in Figs. 3–5 support the excellent description of the data by the rotational model in the form of Eq. (5). The fitting parameter $I_f$ may consist of two constants, level spin $I$ and the alignment at rotational frequency $\omega=0$, $i_0$, which cannot be distinguished in the least-squares procedure. Level spin is quantized, and therefore the magnitude of $i_0$ can be examined modulo (half) integer through a study of the quantity $\Delta$ defined earlier, tabulated in Tables I and VII, and illustrated in Fig. 2. Table VII lists the value of $\bar{\Delta}$ and $\Delta_{\rm rms}$ for the even-even, odd-$A$, odd-odd nuclei, as well as the ensemble. For the ensemble of 25 bands, $\bar{\Delta}$ and $\Delta_{\rm rms}=0.041(27)$ and 0.102(19), respectively, and we adopt $\pm 0.1\hbar$ for the uncertainty with which we can determine $\Delta$ (the shaded region in Fig. 2). Therefore a value of $\Delta$ which includes this region is consistent with $i_0$ integer, including 0. Study of Fig. 2 shows that $I_f$ is within this region for all nine bands of the even-even nuclei, for 7 of the 10 odd-$A$ bands, for two of six odd-odd bands, and in aggregate, for 18 of the 25 bands. The error bars on the points for $^{192}$Pb(1) and $^{195}$Tl(1,2) are very large although they are included in tables and the discussion.

### 1. *Even-even nuclei*

Consider the even-even nuclei. The values of $\bar{\Delta}$ and $\Delta_{\rm rms}$ for the nine SD bands given in Table VII are $0.034(31)\hbar$ and $0.085(15)\hbar$, respectively. Alignment is expected to approach 0 as $\omega$ approaches 0 for these nuclei, and it is not quantized in general. The simplest interpretation is that $i_0=0$ and $I_f$ represents level spin $I$ directly. Any other interpretation requires a special mechanism which produces $i_0\neq 0$ for the even-even nuclei listed in Table I. We do not think this alternative is likely and no example has ever been given.

### 2. *Odd-A nuclei*

For the 10 SD bands reported in odd-$A$ nuclei, $\bar{\Delta}$ and $\Delta_{\rm rms}$ are $-0.009(83)\hbar$ and $0.189(54)\hbar$, respectively, and individual values of $\Delta$ are within $0\pm 0.1\hbar$ for 7 of the 10 odd-$A$ SD bands. Again, the simplest interpretation is that $i_0=0$ and $I_f=I$. The exceptions are $^{189}$Hg(1), $^{191}$Hg(1), and $^{195}$Tl(1), where the minimum in $I_f$ lies near

an integer rather than the expected half-odd integer. [The minimum for $^{195}$Tl(2) also is nearer integer; however, within the large errors, $\Delta$ includes $0\pm0.1$.] The $^{189}$Hg(1) and $^{191}$Hg(1) bands depopulate at $E_\gamma=366.0$ and 350.6 keV, respectively, relatively high in transition energy. The band $^{191}$Hg(3) also depopulates at a high transition energy, 311.8 keV, but it still is one transition further down the cascade than the two bands mentioned above. The standard analysis suggests $I=(\frac{29}{2},\frac{31}{2})$ for $^{189}$Hg and $^{191}$Hg, with a slight preference for $\frac{29}{2}$. The statistical accuracy of the $\gamma$-ray energy measurements is somewhat better for the $^{191}$Hg cascade than for the $^{189}$Hg cascade. A careful study of the SD $^{191}$Hg transition energies suggests that $\Delta E_\gamma$ is constant rather than decreasing for the first few low-energy $\gamma$ rays in the cascade (Fig. 3 of Ref. [2]). Following the discussion given earlier in Sec. III, repeating the least-squares fit for $^{191}$Hg with only the first five data points results in $I_f=15.34(22)\hbar$, which differs from the Table I value by one unit. No convincing preference seems to emerge for $I_f$ from these considerations. However, analysis in terms of the cranking model discussed in Sec. V C below may provide a guide.

#### 3. *Odd-odd nuclei*

One example of an odd-odd nucleus with SD bands has been reported in this mass region, $^{194}$Tl, and it has six bands. For these bands, $\overline{\Delta}$ and $\Delta_{\rm rms}=0.247(73)\hbar$ and $0.260(64)\hbar$, respectively. Two of the six SD bands in the odd-odd Tl nucleus meet the $\Delta=(0\pm0.1)\hbar$ criterion, while four of the bands have large $\Delta$. Other than calling attention to the large error bars of the measurement, we offer no explanation at this time.

### B. Expectations from systematics

Systematics may offer some guide for the value of $i_0$. Orbitals with high $j$ and low $\Omega$ are most likely to align in this mass region [29]. Alignment of $\sim(5-10)\hbar$ might be possible from pairs of such orbitals for even-even nuclei. This alignment added to $I_f$ would give $I\sim15\hbar$ for the low-energy member of the SD band. This suggests that depopulation of the SD bands would populate states with $I\sim15\hbar$ less a few units of angular momentum carried away by the unobserved linking transitions. However, where measurements have been made, levels of much lower spin are populated. For example [1,20], the average level spin populated by the decay of the SD band in $^{192}$Hg is $\sim8\hbar$. Population of states with spin $>12\hbar$ was not observed. Therefore $I=15\hbar$ seems unlikely for the low-energy state of this SD band. It follows that initial alignment $i_0\sim5\hbar$ is unlikely for $^{192}$Hg(1), as we have pointed out before [1]. Presently the list of nuclei with established coincidence relationships between transitions of the SD band and transitions between first-well levels with $I\sim10$ includes $^{191}$Hg [2,24], $^{192}$Hg [1,20], $^{193}$Hg [15], $^{194}$Hg [19,26], and $^{194}$Pb [12,13]. Thus, we expect that $I\approx15\hbar$ (or more) is unlikely for the low-energy member of all these bands.

Finally, Stephens *et al.* [22] have pointed out that backbending below $\hbar\omega=175$ keV is unknown, and it is even less likely in these nuclei because they are much more deformed than those nuclei for which we have well-developed systematics.

### C. Exceptions from the cranking model

The validity of the assumption that there is no alignment at $\omega=0$ can be studied using cranked-shell-model calculations. Except for $\Omega=\frac{1}{2}$ orbitals, the alignment of all orbitals must approach 0 as $\omega$ approaches 0. A number of cranking-model calculations have been done for these nuclei, and all of them show this feature. For neutrons, the trajectory of the orbitals near $N=110$, e.g., $[642]\frac{3}{2}$, $[512]\frac{5}{2}$, and $[505]\frac{11}{2}$ Nilsson orbitals, is generally quite flat for $\hbar\omega<0.2$ MeV. The orbitals with the most pronounced slope near $N=110$ is $[761]\frac{3}{2}$, but it also has very little slope for $\hbar\omega<0.1$ MeV. Thus, very little alignment due to neutron orbitals is expected below $\hbar\omega=0.2$ MeV in this model. Cranked-shell-model calculations can provide an estimate of the error likely to be made in the identification of $I_f$ with level spin since the data do not exist at low $\hbar\omega$. We choose the orbital with the most slope $(dJ_x/d\omega)$ below $\hbar\omega=0.2$ MeV and extrapolate its trajectory from $\hbar\omega=0.2$ to 0 MeV smoothly from the trajectory for $\hbar\omega>0.2$ MeV. We then estimate the integral of $dJ_x/d\omega$ from $\hbar\omega=0.2$ to $\hbar\omega=0$ MeV based on the extrapolation and compare with the calculated value. The difference provides an estimate of the error in spin that may result because there are no experimental data below $\hbar\omega\approx0.2$ MeV. Cranked Nilsson calculations (without pairing) were used with $\epsilon=0.47$ to make this estimate. The orbital with the most slope near $\hbar\omega=0$ is the $[761]\frac{3}{2}$ orbital mentioned above, which is the same orbit mentioned in connection with the SD band $^{191}$Hg(1) [2]. We use this orbit as a worst case, and find a difference of $\approx0.5\hbar$ between calculated $dJ_x/d\omega$ and extrapolation. Thus, if the low-frequency cutoff in the experimental data is $\hbar\omega=0.1$ MeV, no error in the spin is expected, while if the low-frequency cutoff in the data is $\hbar\omega=0.2$ MeV, the error is no worse than $\frac{1}{2}\hbar$. This calculation at the same time accounts for the behavior of the $^{191}$Hg(1) cascade at the lowest frequencies observed and the least-squares value $I_f=14.87(7)\hbar$ for this odd-$A$ nucleus, provided both the orbital identification and data are correct. (The data and fit have been discussed in Sec. III.) The magnitude of the calculated alignment ($\approx\frac{1}{2}\hbar$) and its sign (+), combined with the least-squares value of $I_f$, suggest that the spin of the low-energy state in the 350.6-keV transition is $\frac{31}{2}$. If this orbital is also responsible for the $^{189}$Hg(1) cascade (as has been suggested), then the calculation also suggests that the spin of the low-energy member of the $^{189}$Hg(1) cascade is $\frac{31}{2}\hbar$. Tilted-axis cranking model or particle-rotor model calculations may lead to significantly larger effects, especially for intruder orbitals.

### D. Moments of inertia

Values of $\alpha$ and $\beta$ calculated with (half-) integer $I_f$ corresponding to the least-squares minima are listed in Table

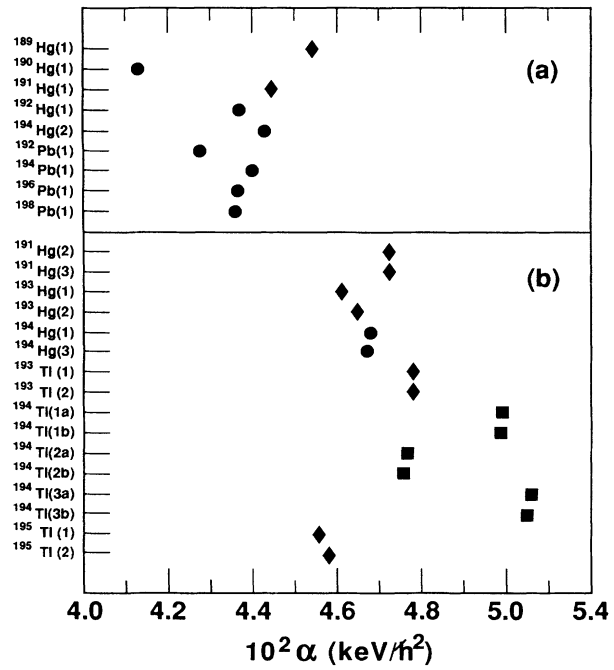


FIG. 7. The least-squares parameter $\alpha$ obtained from a fit of the SD cascade transition energies to Eq. (5) with $I_f$ held constant at the (half-) integer value nearest the minimum of the full least-squres fit. Parameters for SD bands without an observed signature partner are given in (a), and those bands with a signature partner are given in (b). Parameter values are summarized in Table II. Values for even-even, odd-$A$, and odd-odd nuclei are symbolized by ●, ♦, and ■, respectively. Errors are less than the size of the plotted symbol. See Table I for references to the experimental data.

II. They have substantially reduced errors compared to the values listed in Table I because $I_f$ is fixed. These values of $\alpha$ are illustrated in Fig. 7, and they show some correlations. Bands identified as signature partners with small signature splitting have values of $\alpha$ equal within $\frac{1}{4}\%$ or less (except for $^{193}$Hg), supporting that identification. All three Tl bands have distinct values of $\alpha$, a nucleus where the distinction between yrast and excited bands is less clear. Values of $\alpha$ are distinct for the yrast band and the excited bands, e.g., $^{191}$Hg and $^{194}$Hg. Values of $\alpha$ for bands with and without observed signature partners show a clustering, as the list in Table II shows. On average, the moment of inertia is expected to increase as $A^{5/3}$ as nucleons are added. The expectation, therefore, is that the moment of inertia should change by 5.3% from $^{192}$Pb to $^{198}$Pb; the largest difference is considerably less, 2% between $^{192}$Pb and $^{194}$Pb, and $\alpha$ is constant within 1% for $^{194}$Pb, $^{196}$Pb, and $^{198}$Pb. Values of $\alpha$ can be compared with values predicted using the results of fully self-consistent microscopic Hartree-Fock calculations by Krieger *et al.* [30], and by Delaroche *et al.* [31].

## VI. ALIGNMENT

Many of the SD cascades in the $A=194$ region have equal $\gamma$-ray energies within a few parts per thousand, a startling result. Equal $\gamma$-ray energies require quantized alignment (integer, including 0). We have suggested [5–7] that many of these bands show alignment $i$ of $1\hbar$ unit relative to $^{192}$Hg or $^{193}$Tl for $\hbar\omega > 0.20$ MeV using the spin assignments summarized here. This is a surprising result. The case of SD $^{194}$Hg has been widely discussed and we use it as a specific example. The alignment of the excited SD bands of $^{194}$Hg [$^{194}$Hg(1,3) or $^{194}$Hg(∗)] relative to SD $^{192}$Hg has been presented in detail, e.g., Fig. 3, Ref. [5]. Above $\hbar\omega=0.20$ MeV, the alignment of $^{194}$Hg(∗) relative to $^{192}$Hg is constant at $1.00(4)\hbar$, a result interpreted by us as quantized alignment of $1\hbar$. Below $\hbar\omega=0.20$ MeV, the alignment exhibits a smooth trend toward the required $i=i_0=0$ at $\hbar\omega=0$. There are no data below $\hbar\omega=0.13$ MeV, where $i\sim 1/2\hbar$.

This alignment plot and our conclusions have generated some controversy. Discussion has focused on the spin assignments, with the suggestion that they are wrong because alignment at $\omega=0$ was not properly considered. Wu *et al.* argue that our assignments are uncertain by $\pm 2\hbar$, contending that spin assignments leading to no alignment are at least plausible as those leading to quantized alignment other than zero. As an example, they shift level spin for $^{194}$Hg(∗) by $1\hbar$ but not $^{192}$Hg. The shift is in such a direction that the alignment of $^{194}$Hg(∗) is $0\hbar$ at $\hbar\omega > 0.20$ MeV. We have presented arguments that the spin assignments given here are correct. However, even if these assignments are wrong in the direction favored by Wu *et al.*, the resulting alignment of $0\hbar$ is still a quantized value, and quite unexpected for a number of reasons. On average, addition of two particles to a "core" results in a larger moment of inertia for the heavier nucleus, corresponding lower transition energies, and therefore reduced (but not 0) alignment is expected. An alignment of $0\hbar$ at $\hbar\omega > 0.20$ MeV has other consequences, since the data below $\hbar\omega=0.20$ MeV would imply negative $i_0$ which must then be accounted for. Orbitals suggested for the SD bands in the $A=194$ region have not included $K=\frac{1}{2}$ orbitals. Even if $K=\frac{1}{2}$ bands are responsible for significant alignment at $\omega=0$, $i_0$, the alignment would not necessarily be integer nor would it be negative. Energetics suggest that $K=\frac{1}{2}$ bands will usually produce positive alignment, contrary to what Wu *et al.* require. Pathological behavior is required for alignment 0 at both $\hbar\omega=0$ and $>0.20$ MeV, since normal band crossings will increase alignment and therefore imply an even lower value at $\omega=0$. Finally, identical bands in even- and odd-mass nuclei can occur when the decoupling parameter $a=1$ in the asymptotic limit. Identical bands in adjacent even-mass nuclei can occur for a two-particle excitation involving two $K=\frac{1}{2}$ bands, to produce the decoupling parameter $a=2$ in the asymptotic limit. One $K=\frac{1}{2}$ band combined with another $K\neq\frac{1}{2}$ orbit will not produce the desired effect, since as pointed out above, most orbitals near the Fermi surface have slope $dJ_x/d\omega=0$.

## VII. SUMMARY

There are now 27 SD bands in 13 nuclei in the $A=194$ region. Least-squares techniques have been used to fit 25

$\gamma$-ray cascades to rotational model formulas for transition energy which include only first-order correction terms. Two cascades which show backbending were excluded from the fits. Data were fit to an expansion of level spin in odd powers of $\hbar\omega$ and to the expansion of $E$ in powers of $I(I+1)$. The two methods are in broad agreement, but the expansion in powers of $\hbar\omega$ converges faster. Excellent fits were obtained for 25 bands over an angular momentum range of at least $18\hbar$. As a result, inertial parameters and a spin parameter $I_f$ were obtained. Detailed illustrations and discussions of the fits were presented for bands in $^{191}$Hg, $^{192}$Hg, and $^{194}$Hg. The parameter $I_f$ is (half) integer within $\pm 0.1\hbar$ for 18 of the 25 bands. Arguments were presented to support identification of $I_f$ with $I$, especially for the even-even nuclei. Estimates based on cranked-shell-model calculations suggest that in the worst case, an error of no more than $\sim\frac{1}{2}\hbar$ is expected in identifying $I_f$ with $I$ for orbitals likely to be involved. The same calculations suggest that if the orbit identification is correct for $^{191}$Hg(1), the 350.6-keV transition corresponds to a $\frac{35}{2}\rightarrow\frac{31}{2}$ transition. The assignments depend on the assumption that $i\rightarrow 0$ as $\omega\rightarrow 0$. Spin assignments independent of reaction mechanism and nuclear model are of course desirable, but the method presented here is the best presently available.

Alignment plots obtained with these spins show that many of these nuclei exhibit integer alignment with respect to either $^{192}$Hg or $^{193}$Tl above $\hbar\omega=0.20$ MeV. For example, $^{194}$Hg(*) has $1\hbar$ unit of alignment at high $\hbar\omega$, and we have interpreted this as evidence of quantized alignment. This conclusion has been questioned, and attention has focused on the spin determinations. Strong evidence has been presented here in favor of the spin assignments used to make the alignment plot. However, even if the spin assignments are wrong, the observation of quantized alignment remains. The occurrence of identical transition energies requires not only the same $\mathcal{J}^{(2)}$ but also a quantized alignment (including the possibility of 0). However, if the quantized alignment is 0, then either $i_0=-1$ or there must be irregular behavior in 13 bands at frequencies below $\hbar\omega=0.1$ MeV. We know of no reasonable argument in terms of present nuclear models to account for $i_0=-1$, or for the pathological behavior that would be required for the alignment to curve back to 0 at $\hbar\omega=0$. Finally we conclude by noting that the quantized alignment issue is independent of the spin assignments; the concept of incremental alignment [6] is all that is required to demonstrate quantized alignment for many SD nuclei near $A=194$. The SD bands in the $A=194$ region are leading us toward new physics. There is no ready explanation for the identical or related energies of the SD cascades found in some cases, or for the phenomena of quantized alignment. Spin assignments to these bands are basic for detailed discussion and understanding.

## ACKNOWLEDGMENTS

Nirabendu Roy made the initial observation that the properties of the SD cascade in $^{192}$Hg were such that meaningful spin assignments could be made to the levels of the band. This work was supported in part by the U.S. Department of Energy under Contract No. W-7405-ENG-48 (LLNL), in part by the Office of Energy Research, Division of Nuclear Physics of the Office of High Energy and Nuclear Physics of the U.S. Department of Energy under Contract No. DE-AC03-76SF00098 (LBL), and in part by the National Science Foundation (Rutgers).

[1] J. A. Becker, N. Roy, E. A. Henry, M. A. Deleplanque, C. W. Beausang, R. M. Diamond, J. R. Draper, F. S. Stephens, J. A. Cizewski, and M. J. Brinkman, Phys. Rev. C **41**, R9 (1990).

[2] E. F. Moore, R. V. F. Janssens, R. R. Chasman, I. Ahmad, T. L. Khoo, F. L. J. Wolfs, D. Ye, K. B. Beard, U. Garg, M. W. Drigert, Ph. Benet, Z. W. Grabowski, and J. A. Cizewski, Phys. Rev. Lett. **63**, 360 (1989).

[3] E. F. Moore, R. V. F. Janssens, I. Ahmad, M. P. Carpenter, P. B. Fernandez, T. L. Khoo, S. L. Ridley, F. L. H. Wolfs, D. Ye, K. B. Beard, U. Garg, M. W. Drigert, Ph. Benet, P. J. Daly, R. Wyss, and W. Nazarewicz, Phys. Rev. Lett. **64**, 3127 (1990).

[4] J. A. Becker, N. Roy, E. A. Henry, S. W. Yates, A. Kuhnert, J. E. Draper, W. Korten, C. W. Beausang, M. A. Deleplanque, R. M. Diamond, F. S. Stephens, W. H. Kelly, F. Azaiez, J. A. Cizewski, and M. J. Brinkman, in Proceedings of Nuclear Structure in the Nineties II, Oak Ridge, Tennessee, 1990, edited by N. R. Johnson [Nucl. Phys. **A520**, 187c (1990)].

[5] F. S. Stephens, M. A. Deleplanque, J. E. Draper, R. M. Diamond, C. W. Beausang, W. Korten, W. H. Kelly, F. Azaiez, J. A. Becker, E. A. Henry, N. R. Roy, M. J. Brinkman, J. A. Cizewski, S. W. Yates, and A. Kuhnert, Phys. Rev. Lett. **64**, 2623 (1990).

[6] F. S. Stephens, M. A. Deleplanque, J. E. Draper, R. M. Diamond, A. O. Macchiavelli, C. W. Beausang, W. Korten, W. H. Kelly, F. Azaiez, J. A. Becker, E. A. Henry, S. W. Yates, M. J. Brinkman, A. Kuhnert, and J. A. Cizewski, Phys. Rev. Lett. **65**, 301 (1990).

[7] F. Azaiez, W. H. Kelly, W. Korten, F. S. Stephens, M. A. Deleplanque, R. M. Diamond, A. O. Macchiavelli, J. E. Draper, E. C. Rubel, C. W. Beausang, J. Burde, J. A. Becker, E. A. Henry, S. W. Yates, M. J. Brinkman, A. Kuhnert, and T. F. Wang, Phys. Rev. Lett. **66**, 1030 (1991).

[8] C.-L. Wu, D. H. Feng, and M. W. Guidry, Phys. Rev. Lett. **66**, 1377 (1991).

[9] C.-L. Wu, D. H. Feng, and M. W. Guidry, Phys. Rev. Lett. (submitted).

[10] R. A. Wyss and S. Pilotte, Phys. Rev. C **44**, R602 (1991).

[11] A. Bohr and B. R. Mottelson, *Nuclear Structure* (Benjamin, New York, 1975), Vol. 2.

[12] M. J. Brinkman, A. Kuhnert, E. A. Henry, J. A. Becker,

S. W. Yates, R. M. Diamond, M. A. Deleplanque, F. S. Stephens, W. Korten, F. Azaiez, W. H. Kelly, J. E. Draper, C. W. Beausang, E. Rubel, and J. A. Cizewski, Z. Phys. A **336**, 115 (1990).

[13] K. Theine, F. Hannachi, P. Willsau, H. Hubel, D. Mehta, W. Schmitz, C. X. Yang, D. B. Fossan, H. Grawe, H. Kluge, and K. H. Maier, Z. Phys. A **336**, 113 (1990).

[14] M. W. Drigert, M. P. Carpenter, R. V. F. Janssens, I. Ahmad, P. B. Fernandez, E. F. Moore, T. L. Khoo, F. L. H. Wolfs, D. Ye, K. B. Beard, U. Garg, and Ph. Benet, Nucl. Phys. **A530**, 452 (1991).

[15] D. M. Cullen, M. A. Riley, A. Alderson, I. Ali, C. W. Beausang, T. Bengston, M. A. Bentley, P. Fallon, P. D. Forsyth, F. Hanna, S. M. Mullins, W. Nazarewicz, R. J. Poynter, P. H. Regan, J. W. Roberts, W. Satula, J. F. Sharpey-Schafer, J. Simpson, G. Sletten, P. J. Twin, R. Wadsworth, and R. Wyss, Phys. Rev. Lett. **65**, 1547 (1990).

[16] E. A. Henry, A. Kuhnert, J. A. Becker, M. J. Brinkman, T. F. Wang, J. A. Cizewski, W. Korten, F. Azaiez, M. A. Deleplanque, R. M. Diamond, J. E. Draper, W. H. Kelly, A. O. Macchiavelli, and F. S. Stephens, Z. Phys. A **338**, 469 (1991).

[17] T. F. Wang, A. Kuhnert, J. A. Becker, E. A. Henry, S. W. Yates, M. J. Brinkman, J. A. Cizewski, F. Azaiez, M. A. Deleplanque, R. M. Diamond, J. E. Draper, W. H. Kelly, W. Korten, A. O. Macchiavelli, E. Rubel, and F. S. Stephens, Phys. Rev. C **43**, R2465 (1991).

[18] F. Azaiez, W. H. Kelly, W. Korten, M. A. Deleplanque, F. S. Stephens, R. M. Diamond, J. E. Draper, A. O. Macchiavelli, E. Rubel, J. de Boer, M. Rohn, J. A. Becker, E. A. Henry, M. J. Brinkman, S. W. Yates, A. Kuhnert, and T. F. Wang, Z. Phys. A **338**, 471 (1991).

[19] E. A. Henry, M. J. Brinkman, C. W. Beausang, J. A. Becker, N. Roy, S. W. Yates, J. A. Cizewski, R. M. Diamond, M. A. Deleplanque, F. S. Stephens, J. E. Draper, W. H. Kelly, R. J. McDonald, J. Burde, A. Kuhnert, W. Korten, E. Rubel, and Y. A. Akovali, Z. Phys. A **335**, 361 (1990).

[20] D. Ye, R. V. F. Janssens, M. P. Carpenter, E. F. Moore, R. R. Chasman, I. Ahmad, K. B. Beard, Ph. Benet, M. W. Drigert, P. B. Fernandez, U. Garg, T. L. Khoo, S. L. Ridley, and F. L. H. Wolfs, Phys. Rev. C **41**, R13 (1990).

[21] Z. Szymanski, *Fast Nuclear Rotation* (Clarendon, Oxford, 1983).

[22] F. S. Stephens, M. A. Deleplanque, W. Korten, R. M. Diamond, F. Azaiez, A. O. Macchiavelli, J. A. Becker, E. A. Henry, A. Kuhnert, J. A. Cizewski, and M. J. Brinkman, Phys. Rev. Lett. **66**, 1378 (1991).

[23] J. D. Larson, private communication.

[24] M. P. Carpenter, R. V. F. Janssens, E. F. Moore, I. Ahmad, P. B. Fernandez, T. L. Khoo, F. L. H. Wolfs, D. Ye, K. B. Beard, U. Garg, M. W. Drigert, Ph. Benet, R. Wyss, W. Satula, W. Nazarewicz, and M. A. Riley, Phys. Lett. B **240**, 44 (1990).

[25] C. W. Beausang, E. A. Henry, J. A. Becker, N. Roy, S. W. Yates, M. A. Deleplanque, R. M. Diamond, F. S. Stephens, J. E. Draper, W. H. Kelly, J. Burde, R. J. McDonald, E. Rubel, M. J. Brinkman, J. A. Cizewski, and Y. A. Akovali, Z. Phys. A **335**, 325 (1990).

[26] M. A. Riley, D. M. Cullen, A. Alderson, I. Ali, P. Fallon, P. D. Forsyth, F. Hanna, S. M. Mullins, J. W. Roberts, J. F. Sharpey-Schafer, P. J. Twin, R. Poynter, R. Wadsworth, M. A. Bentley, A. M. Bruce, J. Simpson, G. Sletten, W. Nazarewicz, T. Bengston, and R. Wyss, Nucl. Phys. **A512**, 178 (1990).

[27] P. B. Fernandez, M. P. Carpenter, R. V. F. Janssens, I. Ahmad, E. F. Moore, T. L. Khoo, F. Scalassara, I. G. Bearden, Ph. Benet, P. J. Daly, M. W. Drigert, U. Garg, W. Reviol, D. Ye, and S. Pilotte, Nucl. Phys. **A517**, 386 (1990).

[28] J. E. Draper, F. S. Stephens, M. A. Deleplanque, W. Korten, R. M. Diamond, W. H. Kelly, F. Azaiez, A. O. Macchiavelli, C. W. Beausang, E. Rubel, J. A. Becker, N. Roy, E. A. Henry, M. J. Brinkman, A. Kuhnert, and S. W. Yates, Phys. Rev. C **42**, R1791 (1990).

[29] F. S. Stephens, in *Nuclear Structure at High Angular Momentum,* Proceedings of the International School of Physics "Enrico Fermi," Course 69, Varenna, 1976, edited by A. Bohr and R. A. Broglia (North-Holland, Amsterdam, 1977).

[30] S. J. Krieger, P. Bonche, M. S. Weiss, J. Meyer, H. Flocard, and P.-H. Heenen, Nucl. Phys. A (submitted).

[31] J. P. Delaroche, M. Girod, J. Libert, and I. Deloncle, Phys. Lett. B **232**, 145 (1989).

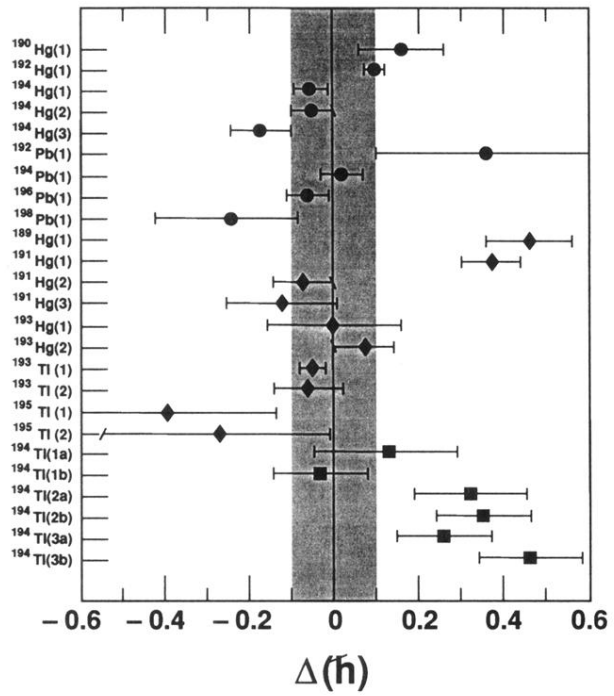


FIG. 2. The values of $\Delta = I_f -$ nearest (half-) integer listed in Table I. They were obtained from the least-squares fit of cascade transition energies to the expression for $I$ as a series in odd powers of $\hbar\omega$ ($= E_\gamma/2$), Eq. (5). Values for even-even, odd-$A$, and odd-odd nuclei are labeled by ●, ♦, and ■, respectively. See Table I for references to the data.

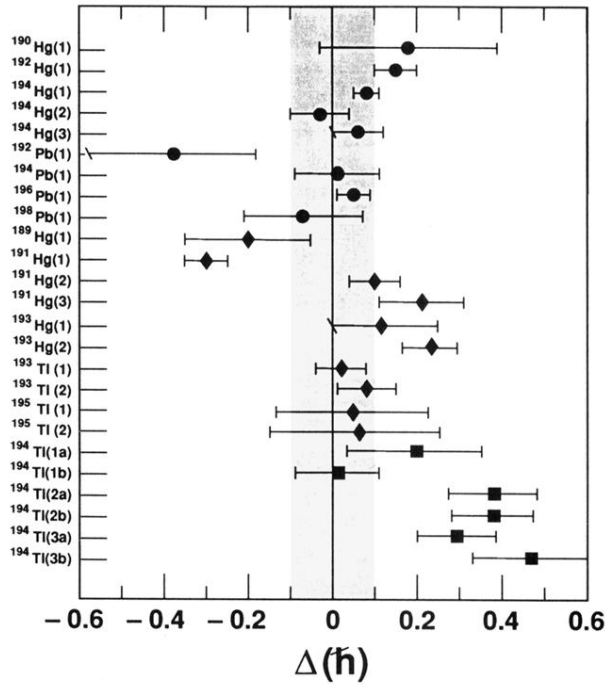


FIG. 6. The quantity $\Delta = I_f -$ nearest (half-) integer listed in Table V. The value of $I_f$ was obtained from the least-squares fit of cascade transition energies to $E(I+2 \rightarrow I) = E(I+2) - E(I)$, with $E(I)$ expressed as a power series in $I(I+1)$, Eq. (2). Values for even-even, odd-$A$, and odd-odd nuclei are labeled by ●, ♦, and ■, respectively. See Table I for references to the data.